J|A|C|S COMMUNICATIONS

Published on Web 06/02/2009

Broadband "Infinite-Speed" Magic-Angle Spinning NMR Spectroscopy

Yan-Yan Hu,[†] E. M. Levin,[‡] and Klaus Schmidt-Rohr*,[†]

Ames Laboratory and Department of Chemistry, Iowa State University, Ames, Iowa 50011, and Ames Laboratory and Department of Physics and Astronomy, Iowa State University, Ames, Iowa 50011

Received April 24, 2009; E-mail: srohr@iastate.edu

Determination of the spectrum of isotropic spectral shifts (chemical, Knight, or paramagnetic shifts) is a central goal of high-resolution NMR. For spin-$^1/_2$ isotopes, magic-angle spinning (MAS) can often achieve this goal, but in some cases spinning sidebands, due to large chemical-shift anisotropies, may obscure the isotropic-shift information. This is a particularly serious problem for high-Z nuclei, such as ^{125}Te, ^{207}Pb, ^{119}Sn, ^{113}Cd, and ^{195}Pt, which have large chemical-shift anisotropies when they are located in low-symmetry (less than cubic) environments. In some cases, even at relatively high-speed MAS the sidebands are still merged; Figure 1 shows that this problem exists in 22-kHz MAS ^{125}Te NMR spectra of various tellurides, several of which have interesting applications as thermoelectrics[1,2] or as phase-change materials for reversible data storage on CDs and DVDs.[3] While the sidebands in the spectrum of Ag_2Te, Figure 1a, are narrow enough to be merely a nuisance, those of Sb_2Te_3 and GeTe (see Figure 1b and c, respectively) are merged due to a broad distribution of isotropic shifts, whose spectrum cannot be determined under these conditions. In the high-performance thermoelectric $Ag_{0.53}Pb_{18}Sb_{1.2}Te_{20}$[2] (Figure 1d), the relative intensity of the smaller band of Te bonded to Sb at −1500 ppm cannot be reliably determined because of overlap from (unresolved) sidebands of the main peak. It appears that similar effects, manifested as no line narrowing in 8-kHz MAS ^{125}Te NMR, were also observed for some transition metal tellurides.[4]

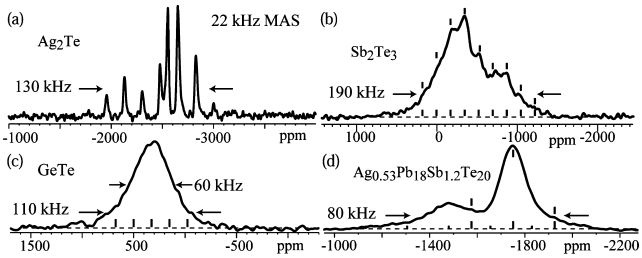

Figure 1. ^{125}Te NMR spectra of several tellurides, at 22-kHz MAS and 9.4 T. (a) Ag_2Te. (b) Sb_2Te_3. (c) GeTe, a phase-change and thermoelectric material. (d) $Ag_{0.53}Pb_{18}Sb_{1.2}Te_{20}$, a high-performance thermoelectric material. Spinning sideband positions are marked. The homogeneous line width $1/(\pi T_2)$ is <7 ppm.

Faster magic-angle spinning can increase the spacing of sidebands and decrease their intensities. Nevertheless, an often superior approach is complete removal of spinning sidebands by suitable sequences of short radio frequency pulses[5−7] producing a large nutation frequency γB_1, since in most NMR probeheads the maximum γB_1 clearly exceeds the maximum MAS frequency ω_r achievable. For instance, in our probehead with 2.5-mm rotors, $\omega_r < 2\pi$ 35 kHz, while $\gamma B_1 > 2\pi$ 110 kHz.

Various pulse sequences with four or more 180° pulses have been introduced for sideband suppression,[5−7] but due to the length and unfavorable off-resonance properties of 180° pulses, they cannot achieve the broadband excitation required for spectra as in Figure 1 spanning 100 kHz or more. In particular, total suppression of sidebands (TOSS)[5] does not work well in many of these cases, giving very small intensities for sites with large sidebands. The projection of suitably sheared phase alternated spinning sideband (PASS) NMR spectra,[6] obtained with five 180° pulses, can provide quantitative spectra with only minor sidebands and with good sensitivity, but only for moderate ranges in isotropic chemical shifts (<0.7 γB_1).[7] Instead, we have identified Gan's magic-angle turning (MAT) experiment[8,9] with five 90° pulses as a superior alternative; here, the projection after suitable shearing yields the "infinite-speed" spectrum free of spinning sidebands. The MAT experiment provides a larger bandwidth than TOSS or PASS since it requires only four ∼90° pulses in addition to the regular excitation pulse (see Figure 2a). The bandwidth of a 90° pulse is large, >5 γB_1, if the length of the magnetization in the transverse plane is considered, but one needs to account for the nearly linear off-resonance phase shift $\approx \omega_1 t_p/2$.[10] Thus, evolution occurs effectively for about half the pulse duration t_p, as indicated in Figure 2. As a result, a nominal evolution time $t_{1,nom}/2 = 0$ corresponds to an effective evolution time $t_1/2 \approx t_p$ (see Figure 2b). The first slice without evolution, $t_1/2 = 0$, is obtained by omitting the "evolution pulses" altogether (see Figure 2c).

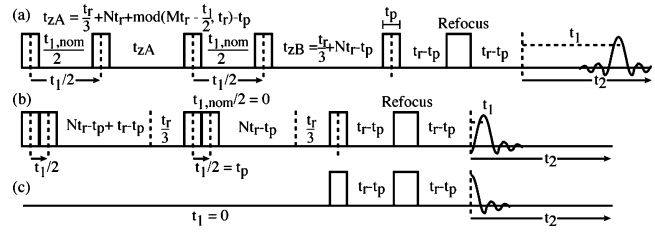

Figure 2. Fast magic-angle turning pulse sequence for broadband complete sideband suppression. (a) General pulse sequence, with two z-periods t_{zA} and t_{zB}. The unequal timings shown are for the "t_1 time reversed" MAT$^-$ data set,[9] while the MAT$^+$ data set is obtained with $t_{zB} = t_{zA}$, both decremented with increasing $t_1/2$ [using a cyclic list from t_r to t_p (pulse duration) in steps of $-t_p$]. Flip angles can be 70° to 90° for the first five pulses and 120°−180° for the last pulse. (b) Pulse sequence for nominal $t_{1,nom}/2 = 0$, but effective $t_1/2 = t_p$. (c) Simplified pulse sequence for $t_1 = 0$.

While MAT has mostly been applied at low spinning frequencies of ∼0.1 kHz to measure site-resolved chemical-shift anisotropies,[8,9] for our purpose fast spinning with frequencies >20 kHz is required to maximize sensitivity, using the MAT $^{\pm}$ approach[9] for solving the 2D phase problem. After shearing by arctan($^1/_2$) along ω_1, by arctan($^{-2}/_3$) along ω_2, and scaling of ω_1' by $^2/_3$, the signal is concentrated in narrow vertical ridges (centerband and spinning sidebands) (see Figure 3a). Summation of vertical slices at these ridges (rather than over a wide range of noise or potential artifacts) gives the desired spectrum without sidebands. Cyclic decrementation

[†] Ames Laboratory and Department of Chemistry.
[‡] Ames Laboratory and Department of Physics and Astronomy.

10.1021/ja903334p CCC: $40.75

of t_{zA} as indicated in Figure 2a keeps t_{zA} and t_{zB} short, avoiding T_1 relaxation and loss of synchronization. Since the time signal of a broad spectrum decays fast, we have added a rotation-synchronized Hahn spin echo before detection, which moves the signal out of the pulse dead time without interfering with rotary refocusing. Compared to a regular 1D spectrum, sensitivity in MAT is reduced by a factor of $\sim 1/4$, because during t_{zA} and t_{zB} only one magnetization component is retained.

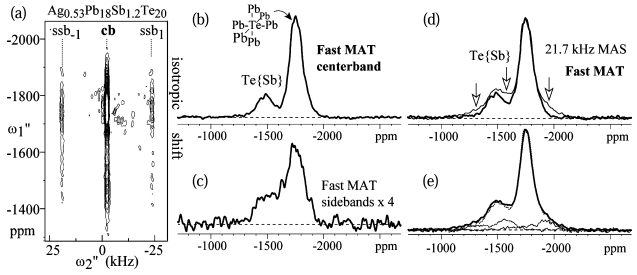

Figure 3. ^{125}Te NMR spectra of $Ag_{0.53}Pb_{18}Sb_{1.2}Te_{20}$. (a) 2D fast MAT spectrum after shearing along ω_1 and ω_2 providing the isotropic shift spectrum along ω_1'' (vertical) and the sideband pattern along ω_2'' (horizontal). Spinning frequency: 21.74 kHz; 80°-pulse length: 2 μs; recycle delay: 150 ms. (b) Centerband slice. (c) Sum of sideband slices, scaled up 4-fold. (d) Comparison of the "infinite-speed" spectrum from fast MAT (thick line, sum of center- and sideband slices) with the regular 21.74-kHz MAS spectrum (thin line). Arrows mark unresolved spinning sidebands in the regular spectrum. (e) Dotted lines (low-intensity bands): First-order sideband slices from MAT at their "natural" positions. Continuous line: regular 21.74-kHz MAS; dashed line: sum of MAT slices. Experiment time: 48 h.

Figure 3a shows a fast MAT 2D ^{125}Te NMR spectrum of $Ag_{0.53}Pb_{18}Sb_{1.2}Te_{20}$ obtained with the pulse sequences of Figure 2 and sheared to provide isotropic shifts along ω_1'' (vertical) and just center- and sidebands along ω_2'' (horizontal). The centerband slice and the sum of first-order sideband slices are shown in Figure 3b and 3c, respectively. Peaks in the sideband slices are broader, most likely due to the greater sideband contribution from sites with larger chemical-shift anisotropies, which usually arise from a more disordered environment. The sum of all three slices is shown in Figure 3d (thick line) and compared with the regular 22-kHz MAS spectrum (thin line). The shoulders labeled by arrows in the regular 1D spectrum are unresolved spinning sidebands. These are seen to significantly increase the apparent signal of Te bonded to Sb around -1500 ppm. As a result, the apparent Te{Sb} fraction in the regular MAS spectrum is 30%, while the actual number from MAT is (22 $\pm$ 3) %. This has important implications for clustering or segregation of Sb in this thermoelectric material.[11,2] For instance, if all Sb was randomly placed on the Pb sublattice independent of Ag, 31% of all Te would have an Sb neighbor and resonate near -1500 ppm; this is clearly not the case, indicating dopant clustering[11] that may improve thermoelectric properties.[4,11] The assignment of the "additional" signal in the 22-kHz MAS spectrum to sidebands is confirmed in Figure 3e, where the contributions from the Nth sideband obtained from MAT are shown (dotted lines) in their "natural" positions, $\omega_{iso} + N\omega_r$. In Figure 3e, the sum of these sidebands and the centerband (dashed line) is also compared with the regular MAS spectrum (continuous line). The good agreement shows that the additional pulses in MAT do not produce significant spectral distortions. The noise could be reduced further by time-domain filtering centered on the echo maximum.

Sb_2Te_3, also a good thermoelectric material,[1] provides an example of a system with a wide spectrum, spanning 2π 170 kHz, due to a large chemical-shift anisotropy reflecting its noncubic, rhombohedral structure.[12] The 2D fast MAT ^{125}Te NMR spectrum of Sb_2Te_3 is shown in Figure 4a, and Figure 4b compares the "infinite speed" MAS spectrum (thick line) obtained from the sum of the fast-MAT signal slices with the regular 22-kHz MAS spectrum (thin line). The sideband suppression greatly narrows the signal and exposes an asymmetry or shoulder to the left of the main peak, which could be due to the central Te layer in the layered Te−Sb−Te−Sb−Te crystal structure.[12] The comparison of the sum of MAT center- and sidebands in their "correct" positions with the regular MAS spectrum (see Figure 4c) confirms that fast MAT works well for large CSAs spanning $\sim 1.5\ \gamma B_1$.

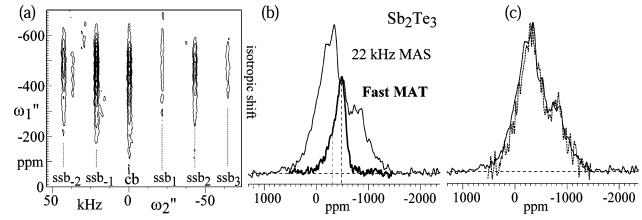

Figure 4. ^{125}Te NMR spectra of Sb_2Te_3. (a) 2D fast MAT spectrum after shearing to provide the isotropic shift spectrum along ω_1'' and the sideband pattern along ω_2''. Spinning frequency: 21.74 kHz; recycle delay: 50 ms; experiment time: 36 h. (b) Thick line: Isotropic chemical-shift spectrum from the sum of the signal slices in (a). Thin line: regular 22-kHz MAS spectrum for reference. (c) Comparison of regular 22-kHz MAS spectrum (continuous line) with the sum of MAT center- and sideband slices in their "natural" positions (dashed).

The fast MAT spectra shown here and recorded on model compounds indicate that off-resonance spectral distortions are tolerable for a spectral range of 1.8 $\gamma B_1 = 200$ kHz $= 1600$ ppm of ^{125}Te in a 9.4-T field. This range in ppm can be extended by (i) higher γB_1 values, which can be achieved in smaller radio frequency coils,[13] or (ii) by measurements at lower B_0 fields, where the spread of frequencies is reduced (fewer Hz/ppm). Both of these changes would be accompanied by signal reduction, so sensitivity limitations will impose the eventual estimated constraint of the spectral range to $\sim$4000 ppm of ^{125}Te or $\sim$6000 ppm of ^{207}Pb.

Acknowledgment. This work was supported by the U.S. Department of Energy - Basic Energy Sciences, Contract No. DE-AC02-07CH11358.

References

(1) Snyder, G. J.; Toberer, E. S. *Nat. Mater.* **2008**, *7*, 105–114.
(2) Hsu, K. F.; Loo, S.; Guo, F.; Chen, W.; Dyck, J. S.; Uher, C.; Hogan, T.; Polychroniadis, E. K.; Kanatzidis, M. G. *Science* **2004**, *303*, 818–821.
(3) Atwood, G. *Science* **2008**, *321*, 210–211.
(4) Orion, I.; Rocha, J.; Jobic, S.; Abadie, V.; Brec, R.; Fernandez, C.; Amoureux, J.-P. *J. Chem. Soc., Dalton Trans.* **1997**, 3741–3748.
(5) Dixon, W. T. *J. Chem. Phys.* **1982**, *77*, 1800–1809.
(6) Antzutkin, O. N.; Shekar, S. C.; Levitt, M. H. *J. Magn. Reson., Ser. A* **1995**, *115*, 7–19.
(7) Vogt, F. G.; Gibson, J. M.; Aurentz, D. J.; Mueller, K. T.; Benesi, A. J. *J. Magn. Reson.* **2000**, *143*, 153–160.
(8) Gan, Z. *J. Am. Chem. Soc.* **1992**, *114*, 8307–8309.
(9) Gan, Z. J.; Ernst, R. R. *J. Magn. Reson.* **1996**, *123*, 140–143.
(10) Garwood, M.; DelaBarre, L. *J. Magn. Reson.* **2001**, *153*, 155–177.
(11) Lin, H.; Bozin, E. S.; Billinge, S. J. L.; Quarez, E.; Kanatzidis, M. G. *Phys. Rev. B: Condens. Matter* **2005**, *72*, 174113/174111−174113/174117.
(12) Anderson, T. L.; Krause, H. B. *Acta Crystallogr.* **1974**, *30*, 1307–1310.
(13) Samoson, A. *Encyclopedia of NMR* **2002**, *9*, 59–64. (a) Janssen, H.; Brinkmann, A.; Van Eck, E. R. H.; Van Bentum, P. J. M.; Kentgens, A. P. M. *J. Am. Chem. Soc.* **2006**, *128*, 8722–8723. (b) Tang, J. A.; O'Dell, L. A.; Aguiar, P. M.; Lucier, B. E. G.; Sakellariou, D.; Schurko, R. W. *Chem. Phys. Lett.* **2008**, *466*, 227–234.

JA903334P